

1 Time-lapse geophysical assessment 2 of agricultural practices on soil 3 moisture dynamics

4
5
6 G. Blanchy^{1,2}, C. W. Watts², J. Richards³, J. Bussell^{3 (formerly),4}, K. Huntenburg¹, D. Sparkes³,
7 M. Stalham⁵, M. J. Hawkesford², W. R. Whalley², A. Binley¹

8
9 ¹Lancaster University, Lancaster, Lancashire LA1 4YW, UK
10 ²Rothamsted Research, Harpenden, Hertfordshire AL5 2JQ, UK
11 ³University of Nottingham, Nottingham, Nottinghamshire NG7 2RD, UK
12 ⁴The Game & Wildlife Conservation Trust, Allerton Project, Loddington, Leicestershire LE7
13 9XE, UK
14 ⁵NIAB CUF, Cambridge, Cambridgeshire, CB3 0DL, UK
15

16 Highlights

- 17 - Time-lapse geophysical surveys can help assess the impact of agricultural practices
- 18 - Cover crops affect soil drying while in place but have no substantial effect on the main crop
- 19 - Traffic-induced soil compaction limits water extraction depths of potato crops
- 20 - The soil electrical conductivity in moldboard plowing decreases faster than in direct drill
- 21 - N levels have significant impact on the soil EC after application but not over a longer term

22 23 Abstract

24 Geophysical surveys are now commonly used in agriculture for mapping applications. High-
25 throughput collection of geophysical properties such as electrical conductivity (inverse of
26 resistivity), can be used as a proxy for soil properties of interest (e.g. moisture, texture,
27 salinity). Most applications only rely on a single geophysical survey at a given time. However,
28 time-lapse geophysical surveys have greater capabilities to characterize the dynamics of the

29 system, which is the focus of this work. Assessing the impact of agricultural practices through
30 the growth season can reveal important information for the crop production. In this work, we
31 demonstrate the use of time-lapse electrical resistivity tomography (ERT) and electromagnetic
32 induction (EMI) surveys through a series of three case studies illustrating common agricultural
33 practices (cover crops, compaction with irrigation, tillage with nitrogen fertilization). In the first
34 case study, time-lapse EMI reveals the initial effect of cover crops on soil drying and the
35 absence of effect on the subsequent main crop. In the second case study, compaction,
36 leading to a shallower drying depth for potatoes was imaged by time-lapse ERT. In the third
37 case study, larger change in electrical conductivity over time were observed in conventional
38 tillage compared to direct drill using time-lapse EMI. In addition, different nitrogen application
39 rates had significant effect on the yield and leaf area index but only ephemeral effects on the
40 dynamics of electrical conductivity mainly after the first application. Overall, time-lapse
41 geophysical surveys show great potential for monitoring the impact of different agricultural
42 practices that can influence crop yield.

43 **1 Introduction**

44 Geophysical methods such as electromagnetic induction (EMI) and electrical resistivity
45 tomography (ERT) are increasingly being used for agricultural applications. ERT enables the
46 generation of an image of the electrical resistivity of the subsurface from measurements made
47 using electrodes in contact with the ground. In contrast, EMI senses the electrical conductivity
48 (the inverse of resistivity) of the ground through inductive signals and thus does not require
49 galvanic contact with the subsurface. Originating, in part, from the mineral and oil exploration
50 industries (Schlumberger, 1920), ERT is now widely used for many shallow near-surface
51 applications. EMI has proved effective for soil salinity mapping (Corwin and Lesch, 2005). It

52 has since been widely used for mapping different soil properties (Doolittle and Brevik, 2014),
53 defining management zone in agriculture (Hedley et al., 2004) or assessing soil structure
54 (Romero-Ruiz et al., 2018). More recently the development of multi-coil EMI instruments has
55 enabled simultaneous measurements at multiple depths, enabling the recovery of the
56 distribution of electrical conductivity of the subsurface as in ERT.

57 Understanding the availability and movement of water in the ground has become a significant
58 driver for many geophysical studies and has led to the field of hydrogeophysics (Binley et al.,
59 2015). Geophysical methods have the capability to characterize properties of soil that
60 influence the flow and storage of soil water making such methods relevant for plant-related
61 application (Jayawickreme et al., 2014; Shanahan et al., 2015; Whalley et al., 2017; Zhao et
62 al., 2019; Cimpoiășu et al., 2020). For more information on other geophysical methods, we
63 redirect the reader to the review of Allred et al. (2008) who illustrate a range of geophysical
64 applications in agriculture, and the broader overview of geophysical methods for proximal soil
65 sensing given by Viscarra Rossel et al. (2011). These reviews focus on static surveys for
66 assessment of soil properties and states, however, there is much greater potential for
67 geophysical methods for characterizing the dynamic state of the subsurface, which is the
68 focus of this study.

69 Soil and water are essential resources for agriculture. However, these resources are
70 endangered by intensive agricultural practices which can impact food security (Amundson et
71 al., 2015). Loss of soil structure due to tillage or compaction can substantially affect the plant
72 water availability and nutrients uptake and impact crop growth. Conservation agriculture
73 practices aim at addressing some of these specific issues and improve and sustain crop
74 production. The FAO (<http://www.fao.org/conservation-agriculture/en/>) define three axes for

75 conservation agriculture: (1) minimum mechanical soil disturbance, (2) permanent soil organic
76 cover and (3) species diversification. The case studies presented in this work concentrates on
77 (1) and (2). More specifically, this paper focuses on the agricultural practices: compaction with
78 irrigation, tillage with nitrogen fertilization and cover crops. This work does not aim at
79 exhaustively detailing each practice but rather at assessing the potential of two popular
80 geophysical methods (ERT and EMI) at monitoring the effects of these different management
81 practices on soil properties and soil water status.

82 Traffic-induced soil compaction can be significant in certain (mainly loamy) soils as the
83 compaction occurs in deeper layers. Over short time scales, compaction reduces the soil
84 porosity making it more difficult for the roots to penetrate and the water to circulate in the soil
85 (Keller et al., 2013), potentially impacting the effectiveness of irrigation practices. We redirect
86 the reader to Hamza and Anderson (2005) and Batey (2009) who review the different
87 agricultural impacts of soil compaction. Soil compaction can also have long-term effects
88 (Keller et al., 2017).

89 Tillage, conventionally moldboard plowing increases the soil porosity but worsens the soil
90 structure. Direct drilling (zero-tillage) offers an alternative to conventional tillage as it prevents
91 major disruption of the soil structure. The structure of the soil plays a key role in making water
92 and nutrients available to the crop and hence can affect crop productivity. While tillage has
93 other major implications for the biological activity of the soil (Hobbs et al., 2008), the case
94 study presented in this manuscript focuses on the comparison of plowing and direct drill
95 treatments on the soil moisture dynamics and nitrogen uptake.

96 Cover crops, usually sown in a sequence with the main cash crop, have many benefits. They
97 can improve the soil structure, increase the availability of organic matter and also prevent the

98 loss of nutrients to depth, among other advantages (Fageria et al., 2005). Deep rooting cover
99 crops can increase the porosity of the soil, hence potentially improving the water availability
100 for the main crop.

101 The impact of these practices on the agricultural ecosystem is often assessed using small
102 sampling volumes over a short time-window. Some methods, such as soil coring or
103 installation of access tubes for soil moisture probes can be destructive for the crop and the
104 soil. In contrast, geophysical methods such as ERT and EMI are minimally invasive and
105 enable repeated measurements without disturbing the growth of the crop. The other
106 significant advantages of geophysical methods are their large sampling volume and their
107 high-throughput data collection making them well suited to study field-scale processes.

108 All these advantages make geophysical methods attractive for obtaining a quick single scan
109 survey of the field. This single mapping approach is widely used today and even commercially
110 available for obtaining a proxy textural map for precision agriculture. However, such an
111 approach is not well suited to study highly dynamic soil-plant-water interactions. Instead of a
112 single survey, we argue that geophysical time-lapse monitoring can bring more information
113 about how the agricultural practices influence the soil-plant-water interactions and how this
114 can impact crop productivity.

115 Through a series of case studies, this manuscript aims to demonstrate the potential of time-
116 lapse geophysical investigation to better understand the impact of these practices on the soil
117 moisture dynamics. Specifically, the manuscript aims to:

118 - highlight the potential of time-lapse geophysical surveys to assess conservation agricultural
119 practices;

120 - detail the current limitations of the approach;

121 - provide recommendations on the use of time-lapse geophysical monitoring.

122 **2 Materials and methods**

123 **2.1 Geophysical properties**

124 Geophysical methods measure geophysical properties which are then linked to soil properties
125 of interest using pedophysical relationships (Archie, 1942; Waxman and Smits, 1968;
126 Rhoades et al., 1976; Laloy et al., 2011; Wunderlich et al., 2013; Boaga, 2017). ERT
127 measures the soil electrical resistivity using galvanic coupling and EMI measures the soil
128 electrical conductivity (EC) using inductive coupling. The soil EC (or resistivity) is influenced
129 by many factors such as soil temperature, soil moisture, pore water EC, soil texture and
130 porosity. This makes the interpretation of EC values challenging as the user needs to identify
131 the dominant factor influencing EC for a given site and account for effect of the other ones.
132 This also emphasizes the need for site-specific relationships (e.g. Calamita et al., 2015).

133 The time-lapse approach can help here as some factors are usually relatively constant during
134 the survey time such as soil texture and porosity. Soil temperature can be corrected for (Ma et
135 al., 2011) and in a non-saline rainfed environment the EC of the pore water can often be
136 assumed to remain constant except when fertilizers or other chemicals are applied. Thus, the
137 soil moisture is often the main factor controlling the change in EC observed over the growing
138 season of a crop.

139 **2.2 Electrical resistivity tomography**

140 Electrical resistivity tomography uses multiple electrodes to measure the distribution of the
141 electrical resistivity of the subsurface. In the case studies of this manuscript, all electrodes are

142 located on the surface, but other configuration might involve borehole electrodes, hence
143 increasing the sensitivity of the measurements at depth. ERT measurements are made using
144 four electrodes: a quadrupole. Current is injected between two electrodes and the difference
145 in electrical potential is measured between the other two. Each measurement provides an
146 apparent resistivity, i.e. the resistivity of an equivalent homogeneous subsurface. Given
147 multiple combinations of current and potential electrodes along a transect, a 2D image of the
148 true resistivity can be reconstructed using inverse modeling (Binley, 2015). For a more
149 detailed review on ERT methods in soil science, the reader is directed to Samouëlian et al.
150 (2005).

151 **2.3 Electromagnetic induction**

152 EMI instruments use electromagnetic induction principles to measure the apparent electrical
153 conductivity (ECa) of the subsurface. By making measurements with different induction coil
154 spacing and/or orientation, it is possible to sense different depths of the subsurface, and thus
155 like ERT, inverse methods can be used to convert the apparent conductivity measurements to a
156 depth profile of electrical conductivity (McLachlan et al., 2020; von Hebel et al., 2019). The
157 instrument used in this study is the CMD Mini-Explorer (GF Instruments, Czech Republic),
158 which is composed of one transmitter coil and three receiver coils and can be used in
159 horizontal co-planar (HCP) or vertical co-planar (VCP) orientation. When measuring, the
160 transmitter coil emits a primary time-varying electromagnetic field that induces eddy currents
161 proportional to the ground EC. These eddy currents, in turn, induce a secondary
162 electromagnetic field. Both primary and secondary electromagnetic fields are sensed by the
163 receiver coils. From their ratio, a depth-weighted, “apparent”, electrical conductivity (ECa) can
164 be derived. The larger the separation between the transmitter and the receiver coil, the

165 deeper the volume investigated. The combination of HCP/VCP orientations and the three coils
166 separations enables the collection of up to six data points per sampling location with the CMD
167 Mini-Explorer. In the rest of the manuscript coil configuration will be presented as VCP0.32
168 with VCP the orientation and 0.32 the coil separation in meters. We redirect the reader to
169 Callegary et al. (2007) for more information on the specific aspects of EMI measurements.
170 The inverted change in EC profiles presented in this manuscript were obtained using a
171 Gauss-Newton approach following Whalley et al. (2017), implemented in the open-source
172 code EMagPy (McLachlan et al., 2020).

173 The ECa maps provided by the EMI instruments are often qualitative, showing areas of higher
174 EC and lower EC. While this does not have any impact for mapping applications, its effect is
175 significant for quantitative application. Different methods exist to calibrate apparent EMI
176 values based on independently measured depth profiles of EC. Trenches and soil samples
177 can be used to build an EC depth profile. In this study, EMI calibration was done using the
178 inverted EC values from an ERT transect (Lavoué et al., 2010; von Hebel et al., 2014). Other
179 methods such as using multi-elevation measurements have also been proposed to calibrate
180 EMI data (Tan et al., 2019). von Hebel et al. (2019) reviewed the best practices for calibration,
181 conversion and inversion of EMI data.

182 **2.4 Time-lapse approach**

183 A one-time geophysical survey is useful for assessing the static soil properties but when
184 assessing dynamic states, such as soil moisture, the time-lapse approach is more
185 appropriate. The time-lapse approach consists of multiple surveys taken at different times
186 during the period of interest, e.g. the growing season of a crop. A reference survey, usually
187 chosen as a 'wet' or 'dry' reference, is subtracted from the other surveys to obtain a change in

188 EC. This way, static effects on soil EC (e.g. from texture) is accounted for and only the
189 dynamic part of the EC is analyzed. In non-arid conditions, one of the major drivers of the
190 change in EC observed through the season is the change in soil moisture. Since rainfall
191 events can induce sudden increases in soil moisture, when surveys are focused on assessing
192 changes due to evapotranspiration field measurements should be conducted following
193 significant rainfall events to avoid sensing localized changes in soil moisture.

194 Note that the EC (and hence resistivity) is sensitive to temperature and hence a temperature
195 correction is needed for proper interpretation of a time-lapse survey (Hayashi, 2004; Ma et al.,
196 2011). In this study, ECa values were corrected using:

$$197 \quad EC_{25} = \frac{EC_T}{1+0.02 \times (T-25)}, \quad (1)$$

198 where EC_{25} is the temperature corrected EC (at 25 degrees Celsius) and T is the soil
199 temperature in degrees Celsius. When soil temperature profiles were available (all studies
200 except the compaction case), a depth-weighted temperature was computed using the
201 cumulative sensitivity function of the EMI instrument (Blanchy et al., 2020b). This ‘apparent’
202 temperature was then used in Equation 1 to correct the ECa values.

203 **2.5 Experiments**

204 To demonstrate the potential of time-lapse geophysics to study the impact of different
205 agricultural practices, three case studies with different crops were selected (Figure 1). The
206 first one focuses on the impact of cover crops on the soil moisture availability for the main
207 crop (sugar beet). It also compares short-term and long-term cover crops (Figure 1a). The
208 second case focuses on the impact of soil compaction with two different irrigation treatments
209 on the water uptake of potatoes (Figure 1b). The third case explores the interactions between

210 two types of tillage (moldboard plowing and direct drill) and different application rates of
211 nitrogen fertilizer on winter wheat (Figure 1c).

212

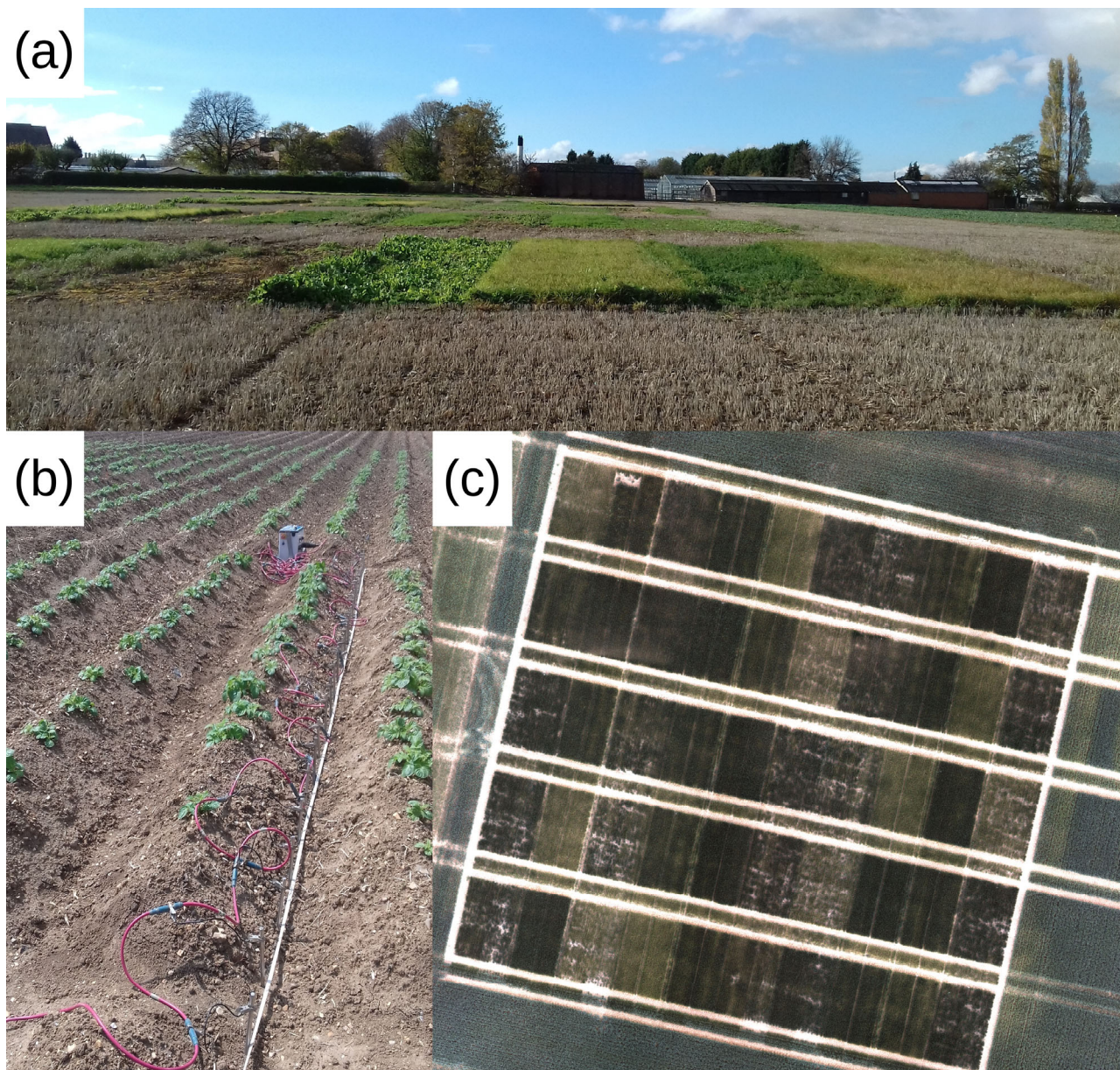


Figure 1: (a) Long-term cover crop experiment (picture taken on 2018-10-29). (b) Compaction experiment on potatoes showing an ERT measurement taking place in a furrow. (c) Experiment on the effects of tillage and nitrogen treatment on winter wheat.

213

214 **2.5.1 Cover crops**

215 Two experiments were carried out with cover crops aiming at assessing the impact on the
216 cover crops on soil moisture availability for the main crop. Cover crops are usually sown in
217 autumn after the harvest of the main crop. They are kept over the winter and, if needed, are
218 destroyed in spring before sowing of the main crop. The hypothesis behind these experiments
219 is that cover crops will improve the soil structure via its root system. The improved soil
220 structure will then help the following cash crop (in this case: sugar beet, *Beta vulgaris* L.) to
221 better access soil moisture. Time-lapse EMI was used to monitor the potential effect of the
222 cover crops on the dynamics of soil moisture.

223 The first experiment was sown with the different cover crops in September 2016 at
224 Nottingham Sutton Bonington campus (52°50'12.4"N 1°15'05.7"W) on a Cambisol (WRB) with
225 a texture of 13.2% clay, 19.5% silt and 67.3% sand. The cover crops were sown in a random
226 block design of four blocks with eight plots (3 m by 7.5 m) per block. Seven different cover
227 crops were tested: oil radish (*Raphanus sativus* L.), tillage radish (*Raphanus sativus* L.),
228 forage rye (*Secale cereale* L.), black oat (*Avena strigosa* Schreb.), white mustard (*Sinapsis*
229 *alba* L.) and Egyptian clover (*Trifolium alexandrinum* L.). An additional bare soil plot was also
230 part of the treatments as a reference. The cover crops were destroyed in December 2016.
231 Sugar beet was then established using direct drilling in spring of the following year and
232 harvested in autumn. EMI data were collected using the CMD Mini-Explorer (GF Instruments,
233 Czech Republic) on 2016-11-09, 2016-12-08 (a few days after the crop was destroyed), 2017-
234 03-08, 2017-05-11 and 2017-06-22 (all dates expressed as ISO 8601).

235 The second experiment was sown with cover crops in September 2017 in a field near to the
236 first experiment (52°49'53.8"N 1°14'49.3"W), also classified as Cambisol. Its aim was not only

237 to estimate the impact of cover crops on soil moisture availability but also to compare cover
238 crops grown over the winter with cover crops in place for a full season. The experimental
239 design was composed of four blocks with 10 plots per block (12 m by 3 m). Four different
240 cover crops were tested: chicory (*Cichorium intybus* L.), a mix of red clover (*Trifolium repens*
241 L.) and cocksfoot (*Dactylis* spp L.), lucerne (also called alfalfa) (*Medicago sativa* L.) and
242 cocksfoot alone. An additional bare soil treatment was also added as a reference. In
243 September 2017, the five cover crop treatments were applied to five plots inside each block.
244 Wheat was grown on the unattributed plots. In September 2018, after the wheat had been
245 harvested, the five treatments were applied on the remaining plots. As such, each block
246 contained two plots with the same treatment, but one was in place since September 2017 and
247 one since September 2018. Figure 1a shows the experiment in October 2018. At the
248 beginning of March 2019, the cover crops were destroyed, and sugar beet was sown using
249 direct drilling. Sugar beet was harvested in autumn 2019. EMI data were collected on 2017-
250 10-25, 2017-12-08, 2018-03-26, 2018-06-19, 2018-08-01, 2018-10-29, 2019-03-11, 2019-05-
251 14, 2019-06-04, 2019-07-03 and 2019-09-10. EMI data were calibrated using ERT lines
252 collected in another experiment nearby following Lavoué et al. (2010).

253 **2.5.2 Compaction and irrigation**

254 A compacted soil can potentially impede root water extraction and hence lead to water stress
255 for some crops. In this experiment, the impact of soil compaction and irrigation is explored on
256 potatoes. The compaction experiment took place in a field managed by the NIAB Agronomy
257 Centre (52°14'13.4"N 0°05'57.9"E) in Cambridge UK in 2018. Two different treatments were
258 applied: compaction/no compaction and frequent irrigation (wet) /severe deficit irrigation (dry).
259 The experiment was composed of four replicate blocks (16 plots; each 3 m by 4.5 m) planted
260 with potatoes (*Solanum tuberosum* L.), cultivar Maris Piper, at a density of 180 tubers per plot

261 in four rows (15 plants per row). Two extra rows were used as irrigation barriers between the
262 plots. The soil was a sandy loam (67% sand, 27% silt, 13% clay, 2.9% organic matter)
263 Cambisol (WRB). The compaction treatment was applied by successive passes of a tractor-
264 drill-cultivator combination with high pressure, row-crop tyres on soil irrigated to field capacity
265 before the formation of the ridges for tuber plantation. An ERT array of 24 electrodes (0.25 m
266 electrode spacing) was used to collect resistivity transects on all plots of block 3 by putting the
267 electrodes in the furrows between the ridges (Figure 1b). ERT data were collected on 2018-
268 06-12 and 2018-08-03. ERT data were inverted with a background constrained approach
269 using ResIPy (Blanchy et al., 2020a) that makes use of the R2 inverse code (Binley, 2015).

270 **2.5.3 Tillage and N treatments**

271 The experiment aims at analyzing the impact of tillage and nitrogen fertilizer application on
272 the growth of winter wheat and the associated soil moisture dynamics. It took place in a field,
273 named "Pastures" (51°48'28.6"N 0°22'23.6"W) managed by Rothamsted Research
274 (Harpenden, UK). The soil of the field is classified as a Luvisol (WRB) with a clayey loamy
275 texture. On 2018-10-03, the experiment was sown with winter wheat (*Triticum aestivum* L.).
276 The experimental setup is composed of five blocks of ten plots each (6 m by 9 m). Two tillage
277 treatments (direct drilling and conventional plowing) and five different nitrogen fertilizer rates
278 (0, 80, 140, 180, 220 kg N/ha) were applied by hand to each plot in two equal splits on 2019-
279 03-04 and 2019-04-23. The tillage treatment was applied in bands across all the blocks while
280 the nitrogen fertilizers were randomly applied to each plot within a block (Figure 1c). ERT
281 arrays (24 pins, 0.25 m electrode spacing) were installed in four selected plots in the
282 experiment to calibrate EMI measurements following (Lavoué et al., 2010). ERT
283 measurements were collected on 2019-02-05, 2019-04-05, 2019-05-07, 2019-05-24, 2019-
284 06-06, 2019-06-18, 2019-07-09, 2019-07-22 and 2019-08-05. EMI measurements using the

285 CMD Mini-Explorer were collected on 2018-12-07, 2019-02-05, 2019-03-01, 2019-03-04,
 286 2019-03-05, 2019-03-07, 2019-03-11, 2019-03-13, 2019-03-21, 2019-04-05, 2019-04-15,
 287 2019-04-30, 2019-05-07, 2019-05-20, 2019-06-06, 2019-06-18, 2019-07-09, 2019-07-22 and
 288 2019-08-05. The field had a large variability with ECa values ranging from 20 to 45 mS/m.
 289 Analysis of variance (ANOVA) was used to detect significant differences ($p < .05$) between the
 290 treatments.

291 Table 1 summarizes the different experiments, instrument used and processing steps.

292 Table1: Summary of the experiments, devices used and processing steps performed.

Experiments	Devices	Processing steps
Impact of cover crops on soil moisture availability	EMI calibrated with ERT	1. inversion of ERT transects 2. calibration of EMI data with inverted ERT (Lavoué et al., 2010) 3. temperature correction of calibrated ECa (Ma et al., 2011) 4. computing Δ ECa from reference 2017-07-22 5. inversion of Δ ECa (Whalley et al., 2017)
Impact of compaction and irrigation on potatoes water uptake	ERT	1. inversion of ERT transects 2. temperature correction of the inverted profiles (Ma et al., 2011) 3. computing Δ ECa from reference 2019-03-11
Impact of tillage and nitrogen fertilization on soil drying under winter wheat	EMI calibrated with ERT	1. inversion of ERT transects 2. calibration of EMI data with inverted ERT (Lavoué et al., 2010) 3. temperature correction of calibrated ECa (Ma et al., 2011) 4. computing of Δ ECa from reference 2018-06-12

293

294 **3 Results**

295 **3.1 Cover crops**

296 Figure 2 shows the evolution of the soil ECa (both apparent Figure 2a and inverted Figure 2b,
 297 c and d) for three selected cover crops and the bare soil treatment in 2016-2017. There is

298 clear difference in ECa in November 2016 with higher values implying greater soil moisture
 299 content. The plots with tillage radish and white mustard exhibit significantly lower apparent
 300 conductivity than the bare soil or the vetch treatments. After the cover crops were destroyed
 301 (mowed) in December 2016, this difference is still visible, but starts to reduce. Finally, in
 302 March 2017, there is no difference between the bare soil and the cover crops treatments.
 303 Similar interpretation can be made using the profiles (Figure 2b, c and d) of inverted change
 304 in conductivity (changes are expressed from July 2017). There are differences between the
 305 bare soil and the cover crops in November 2016 which tend to reduce in December 2016 and
 306 vanish in March 2017.

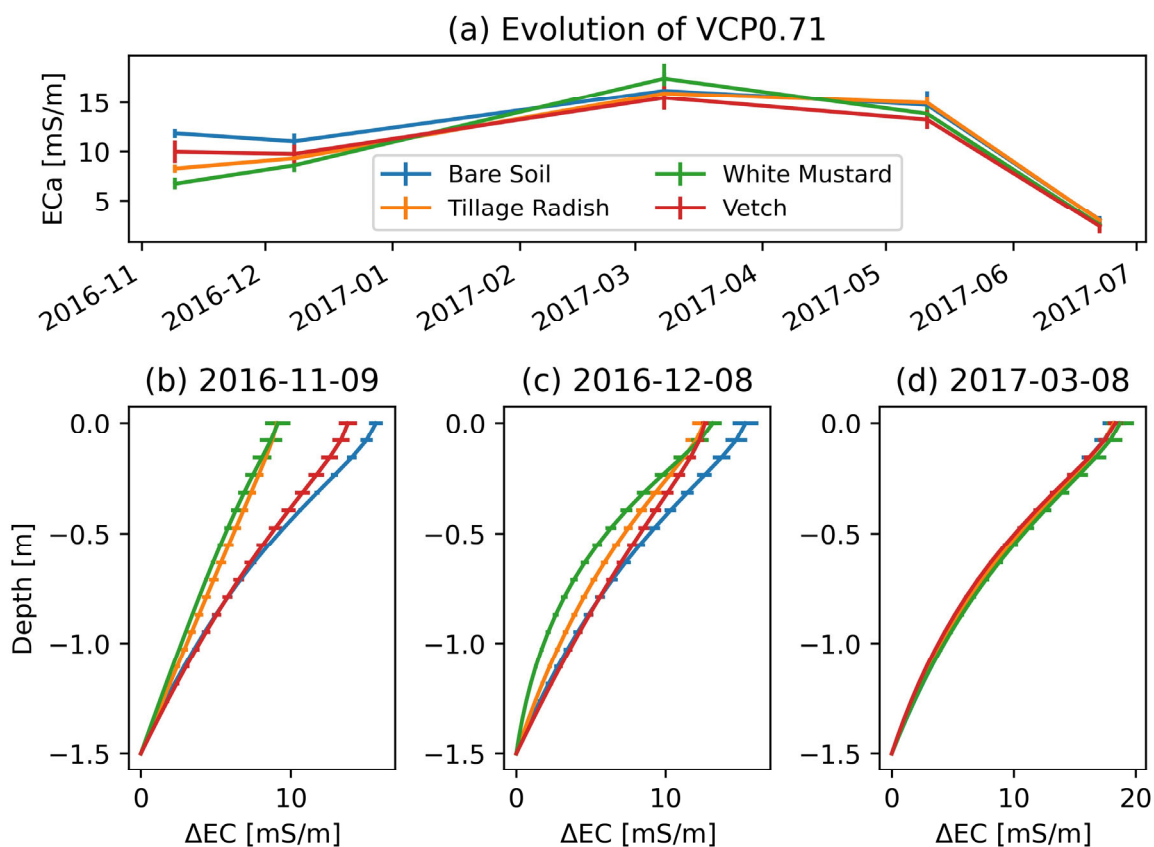


Figure 2: (a) shows the evolution of the apparent electrical conductivity (ECa) for four selected treatments: bare soil, tillage radish, white mustard and vetch. (b), (c) and (d) shows

the inverted change in electrical conductivity (ΔEC) for three different dates. The inverted changes are computed as differences with respect to 2017-07-22 (dry reference).

307

308 Figure 3b shows the evolution of the ECa for the long-term cover crop experiment expressed
309 as differences relative to 2018-03-11. Given the amplitude of the signal in Figure 3b, for each
310 survey date (t), we averaged all differences (ΔECa_t which are still differences from 2018-03-
311 11) from all treatments to form the mean difference ($\overline{\Delta ECa_t}$). For each survey date, this mean
312 was then subtracted from the difference for each treatment. This allows easier comparison
313 between treatments (Figure 3c):

$$314 \quad \Delta ECa_{i,t} - \overline{\Delta ECa_t} = \Delta ECa_{i,t} - \frac{1}{N} \sum \Delta ECa_{i,t}, \quad (2)$$

315 where t is the index of the survey, i is the index of the treatment, N is the number of
316 treatments, $\Delta ECa_{i,t}$ represents the differences relative to 2018-03-11 for treatment i at survey
317 date t , and $\overline{\Delta ECa_t}$ is the mean encompassing all treatments for the survey t .

318 Thus, Figure 3c removes the seasonal trend of Figure 3b and enhances the difference
319 between treatments inside the same survey. The date 2019-03-11 was chosen as a reference
320 because it is the date with minimal effects of the treatments and most homogeneous ECa, all
321 cover crops having been destroyed in the beginning of March. Figure 4 supports Figure 3 by
322 showing subplots of differences in ECa for all varieties. Figure 3 and Figure 4 show data from
323 VCP0.71 (the coil configuration that appears to be the most sensitive to the root zone).
324 However, similar trends, albeit less strong for other coil configurations, can also be observed.
325 Both short-term (sown in September 2018) and long-term (sown in September 2017) cover
326 crops show a significant difference compared to the bare soil treatments (2018-06-19, 2018-
327 08-01, 2018-10-29 in Figure 4). This can be seen over the summer of 2018 (Figure 3a). The

328 long-term cover crops also tend to show a larger difference in ECa compared to the short-
 329 term cover crops (2018-10-29 in Figure 4). For the long-term chicory and lucerne, two deep
 330 rooting cover crops, this difference stays significant even in June and July 2019 but not for
 331 their short-term equivalent. Note that the magnitude of this difference is relatively small (about
 332 2 mS/m) and hence, does not represent a large difference in soil moisture (only a few
 333 percent). The other shallower rooting cover crops, such as the red clover and cocksfoot, do
 334 not show any effect in June or July 2019 for both short and long-term variants.

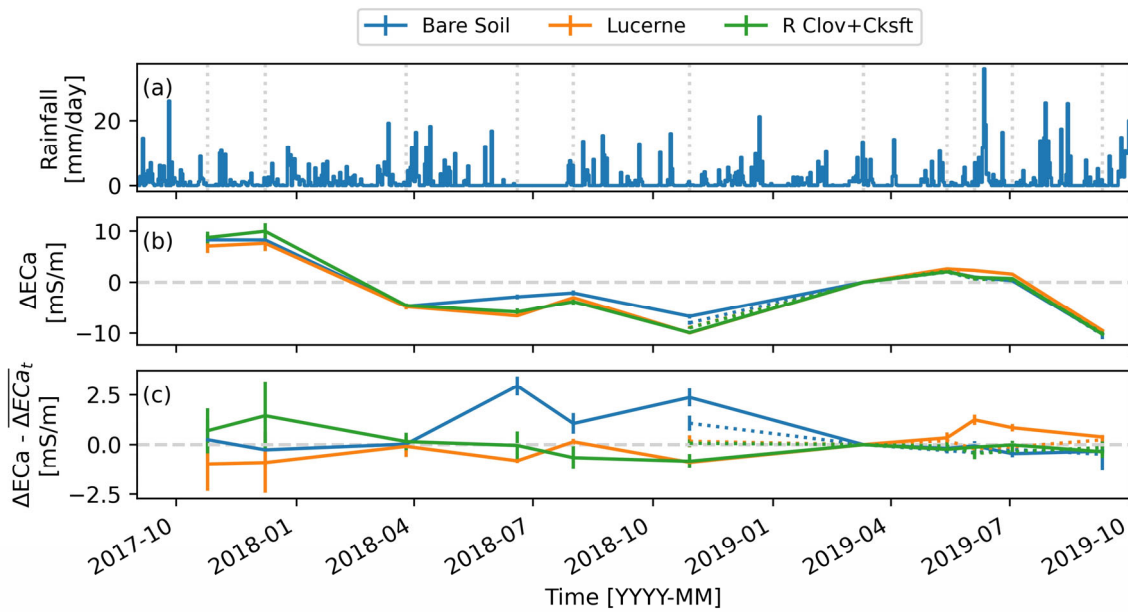


Figure 3: Evolution of the difference in apparent electrical conductivity of VCP0.71 for bare soil, lucerne and red clover + cocksfoot (R Clov + Cksft) treatments in place for one-year (dotted lines) and two years (solid lines). (a) shows the daily rainfall. (b) shows the difference in apparent electrical conductivity compared to the reference date 2019-03-11. To make the difference between treatments more visible, the average difference for all treatments is computed for each survey ($\overline{\Delta ECa}_t$) and is subtracted from (b) leading to (c). Error bars represent the standard error of the mean.

335

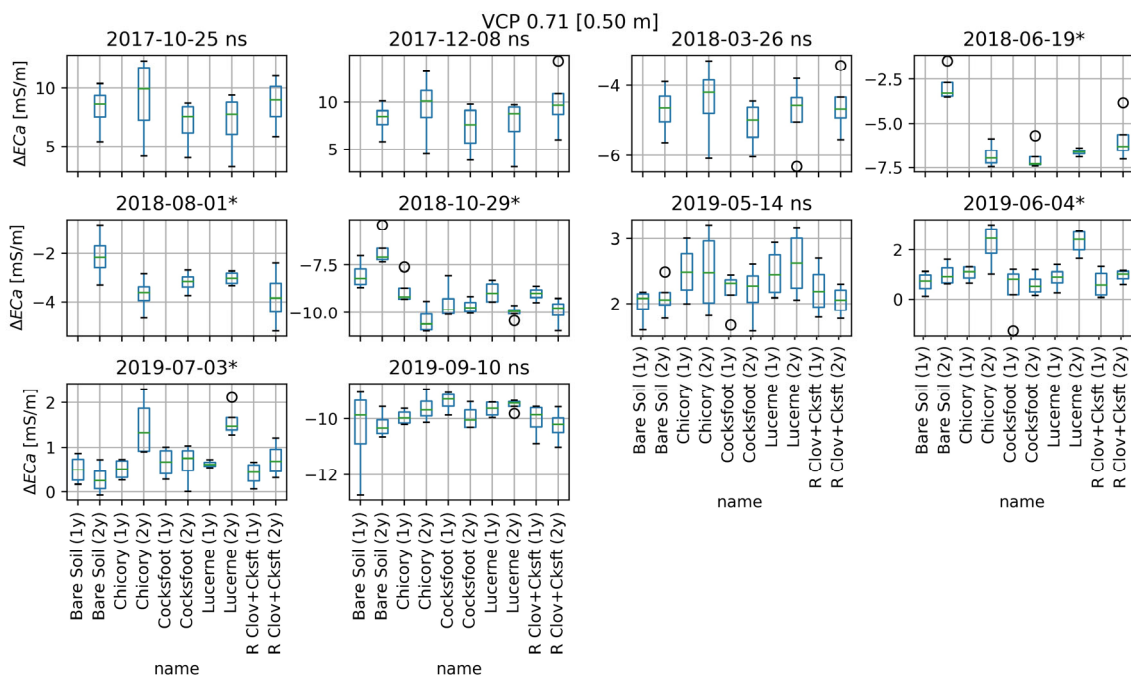


Figure 4: Subplots of boxplots showing the differences in apparent electrical conductivity (ΔECa) compared to the reference date 2019-03-11. Long-term cover crops are indicated by (2y) and short-term by (1y). A star on top of the graph shows that there are significant differences ($p < 0.05$) from an ANOVA test between the treatments. Non-significant results are denoted by 'ns'. Each subplot has its own vertical scale.

336

337 3.2 Compaction and irrigation

338 After inverting each survey, the difference in resistivity from June 2018 to August 2018 ($\Delta\rho$) is
 339 computed and divided by the resistivity of the first survey taken on 2018-06-12 (ρ_0) to obtain a
 340 relative difference. Figure 5 shows the relative difference in inverted resistivity ($\Delta\rho/\rho_0$
 341 expressed as percentage) sections with yellow area associated with an increase in resistivity
 342 (drying) and blue area associated with a decrease in resistivity (wetting). All sections show a
 343 larger positive change, probably associated with soil drying close to the surface, extending no
 344 deeper than 0.7 m. The compacted wet treatment shows the shallowest drying by the crop,
 345 while the non-compacted treatments exhibits deeper drying. Figure 5a and 5c also clearly

346 show the depth of drying is limited, probably by the compaction, compared to non-compacted
347 treatments (Figure 5b and d). No treatments showed any major differences in resistivity
348 deeper than approximately 1.5 m depth.

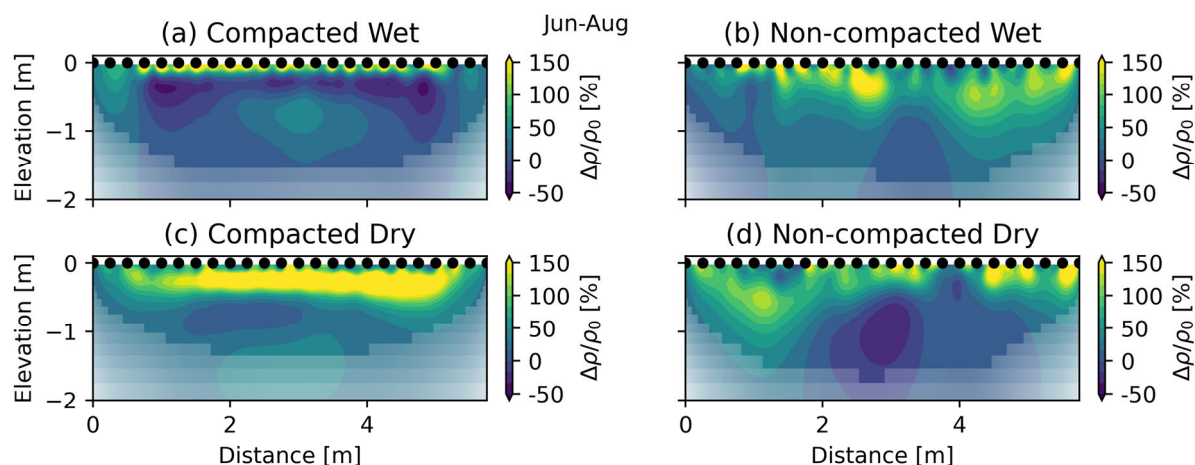


Figure 5: Relative change in inverted resistivity ($\Delta\rho/\rho_0$) section between 2018-06-12 and 2018-08-03 showing the different treatments: (a) compacted wet, (b) non-compacted wet, (c) compacted dry and (d) non-compacted dry. Note that the resistivity is the inverse of the conductivity. The semi-transparent white overlay shows the sensitivity of the survey.

349

350 3.3 Tillage and nitrogen treatments

351 In October 2018, there was a significant ($p < 0.05$ by ANOVA) difference in absolute ECa
352 between the plow and the direct drill treatments prior to any drying by the crops or application
353 of N. The direct drill plots show a higher ECa compared to the plowed plots (data not shown).
354 To remove the effect of this initial difference, the change in ECa is computed by subtracting
355 the values measured on 2018-12-07 (reference date). Figure 6 shows that nitrogen levels
356 only had a significant effect on ECa for a few days following the first fertilizer application
357 where the ECa changes were correlated to the nitrogen rates (Figure 7). The nitrogen
358 fertilizer increases the ECa proportionally to the application rates but because differences in
359 ECa are used and there is a general ECa decrease throughout the season, the inverse

360 relationship is observed. Despite having no significant effect later on in the season, it can still
 361 be observed that the plots which did not receive additional nitrogen fertilizer (0 kg N/ha) are
 362 distinct from the other plots from May onwards in the plow treatment. This cannot be
 363 observed in the direct drill treatment. Figure 8 shows the main effect of tillage treatment. Both
 364 plow and direct drill treatments show a decrease through the season probably related to soil
 365 drying. We observe that the difference between direct drill and plow treatments increases
 366 after the second application of fertilizer for most EMI coil configurations, especially those
 367 which were more sensitive to deeper layers. These differences are not significant anymore
 368 after the 1st July. The nitrogen fertilizer rate had a significant impact on the yield (Figure 9).
 369 Nitrogen fertilizer was more effective at increasing yield in the plow treatment compared to the
 370 direct drill treatment, particularly at the higher rates of N. This effect is also seen in the
 371 development of the leaf area index (LAI) (Figure 10). Between mid-May and mid-June, the
 372 LAI in the direct-drill treatments continues to increase. In the plow treatments, the LAI reaches
 373 its maximum mid-May and does not substantially increase from mid-May to mid-June.

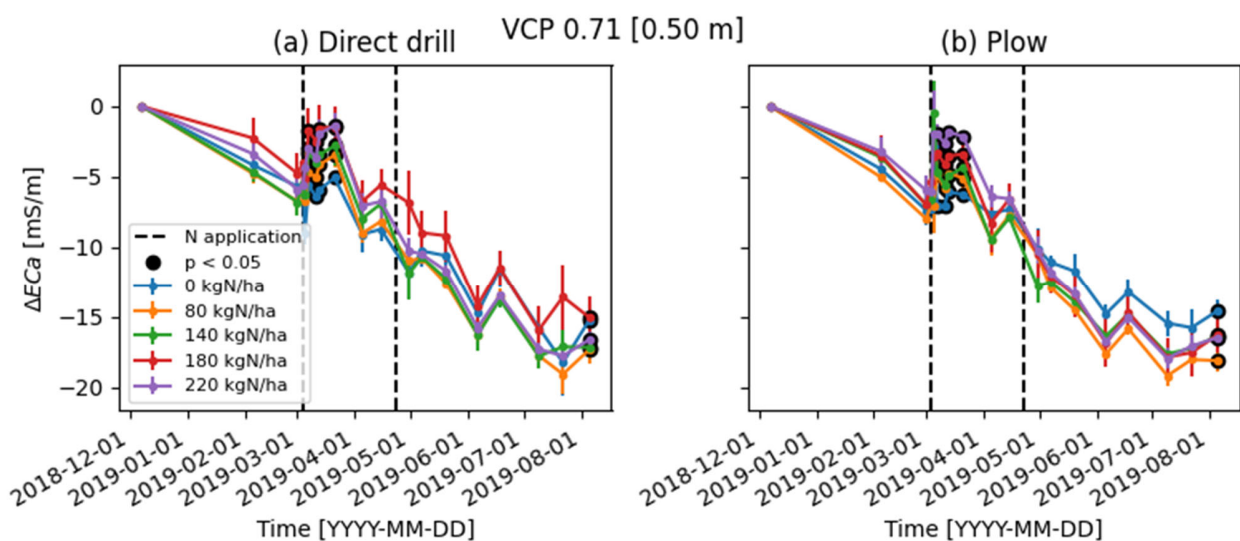


Figure 6: Evolution of the differences in apparent conductivity (ΔECa) for VCP0.71 according

to (a) direct drill and (b) plow treatment. The vertical dotted lines indicate when fertilizer was applied. Black dots show where the difference between the fertilizer treatments is significant ($p < 0.05$ by ANOVA). Error bars represent the standard error of the mean.

374
375

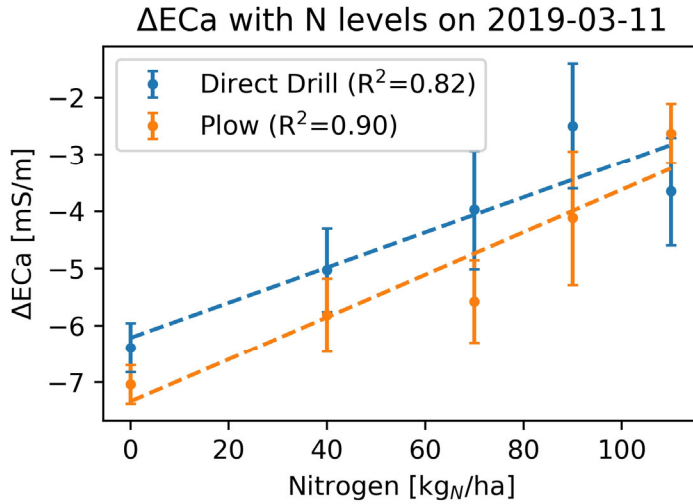


Figure 7: Differences in apparent electrical conductivity (ΔECa) as a function of the amount of nitrogen after the first application (nitrogen applied on 2019-03-04). Note that differences are taken with respect to the reference date 2018-12-07 and not just before the nitrogen application. This is why large amount of fertilizer actually shows a smaller decrease in Eca as they compensate more the global Eca decreases from the reference date.

376
377

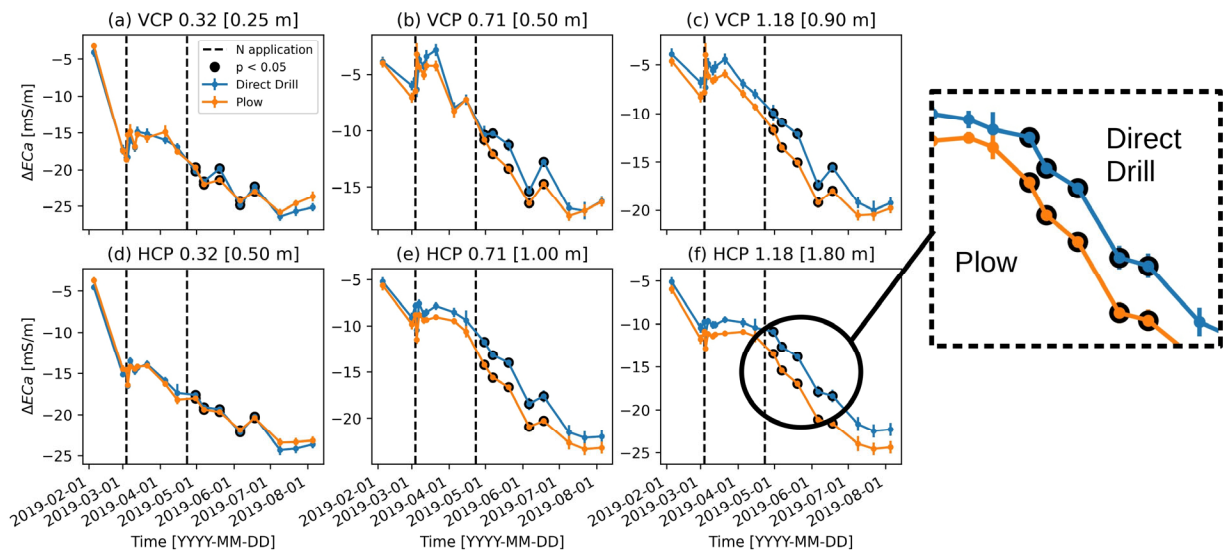


Figure 8: Evolution of the differences in apparent electrical conductivity (ΔECa) with respect to the reference date 2018-12-07 for the six coil configurations of the CMD Mini-Explorer (a to f). All plots have been averaged between direct drill and plow treatment. Error bars represent standard error of the mean. Black dots show where the difference between direct drill and plow treatment is significant ($p < 0.05$ by ANOVA).

378

379

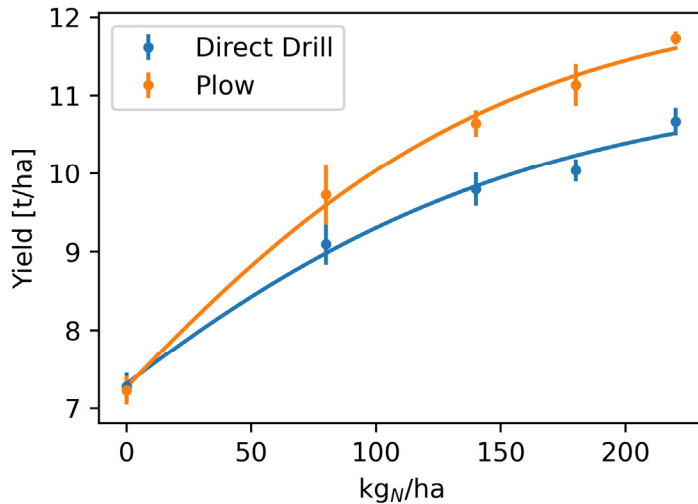


Figure 9: Yield response to the amount of nitrogen fertilizer for the direct drill and plow treatments. Error bars represent the standard error of the mean. A sigmoid ($a/(b+\exp(-c*x +$

d))) has been fitted to both curves.

380

381

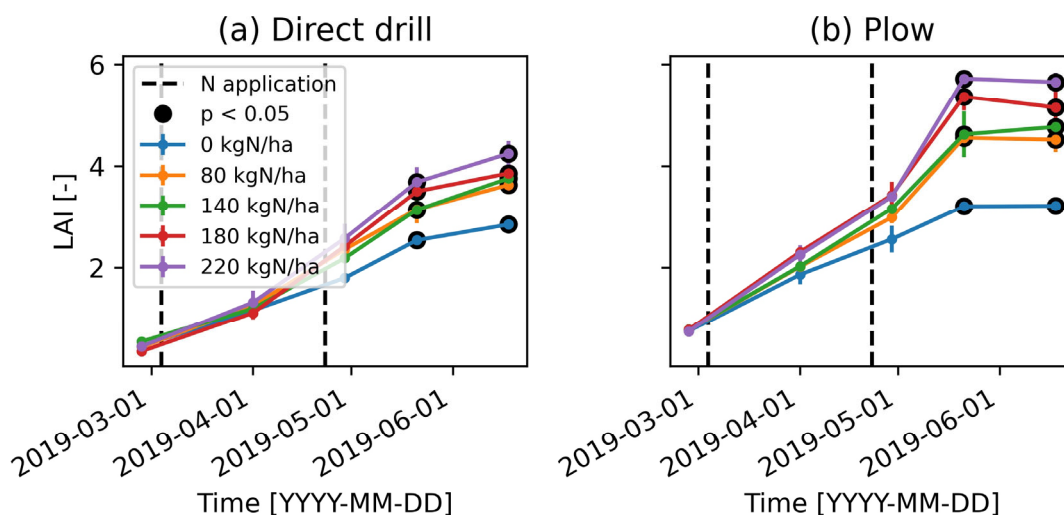


Figure 10: Evolution of the leaf area index (LAI) between direct drill (a) and plow (b) treatments split by amount of nitrogen fertilizers applied. Black dots show where the difference between the fertilizer treatments is significant ($p < 0.05$ by ANOVA). Error bars represent the standard error of the mean.

382

383 4 Discussion

384 4.1 Capabilities

385 A single geophysical survey can be useful to map soil textural variation across the field and, in
386 some cases, can be linked to soil moisture distribution (Calamita et al., 2012). However, there
387 is little information on how it might impact crop productivity. Time-lapse geophysical surveys,
388 in contrast, enable, to some extent, the removal the static effects of soil properties on the
389 geophysical measurements. Changes in EC (or ECa), once temperature corrected, can then
390 more easily be linked to changing states such as soil moisture or pore water ionic
391 concentration. In the case-studies presented here, which took place in non-saline

392 environments, we can reasonably link the changes in ECa to the changes in soil moisture due
393 to crop-water uptake (evapotranspiration). We also observed that during short periods
394 immediately following the application on mineral N, there was a sudden increase in EC
395 probably due to an increase in pore water EC (Figure 6).

396 In the first case study, cover crops were found to have a significant effect compared to the
397 bare soil in the first and second experiments. In November 2016, the tillage radish and white
398 mustard had a larger effect than the vetch. However, after mowing, no more effect of the
399 cover crops on the soil dynamics was observed. In the second experiment, both short-term
400 and long-term cover crops show significant effect compared to the bare soil. Cover crops in
401 place for two years tend to have a larger effect compared to cover crops grown for one
402 season (Figure 4). After being cut down, most cover crop treatments do not show any
403 difference compared to bare soil. Only the long-term chicory and lucerne, two deep-rooting
404 cover crops, show a significant effect in June and July 2019 (Figure 3 and 4). These ECa
405 differences in the long-term chicory and lucerne treatments on 2019-06-04 (Figure 4) could be
406 caused by an improved soil structure allowing better rainfall infiltration and possibly larger
407 moisture storage. Ren et al. (2019) found that white mustard has a positive effect on the soil
408 structure, promoting deeper root penetration of maize crop. However, the magnitude of the
409 change (a few mS/m), once converted to soil moisture only represent a few percent, hence
410 not constituting a substantial difference in soil drying compared to other treatments. Analysis
411 of changes in ECa enhances the differences between cover crops, which would be less
412 obvious with absolute ECa values as part of the signal would be impacted by various soil
413 texture across the field.

414 Potatoes are particularly sensitive to drought stress. While Tang et al. (2019) have attempted
415 to directly related ECa to soil moisture and potatoes tuber yield, the second case study
416 presented here focused on the impact of traffic-induced compaction and irrigation treatment
417 on the soil moisture. Time-lapse ERT between potato ridges reveals the limited depth of water
418 uptake in compacted soil compared to non-compacted treatments. Plants in the non-
419 compacted treatments can probably access water at a greater depth more easily (and thus
420 dry the soil) in comparison to the compacted treatments. In wet treatments, crops rely mainly
421 on the water stored in the uppermost 30-40 cm of soil. One major disadvantage of placing the
422 electrodes in the furrows is that no information can be collected on what is happening inside
423 the ridges. However, this setup enables us to better measure the effect of compaction as all
424 ridges are compaction-free. Such information is potentially useful for agronomists to adapt
425 agricultural practices, such as irrigation-schedules tailored to canopy and root development.
426 Minimally invasive ERT or EMI survey could reveal depth of drying of the crop and help
427 estimate more accurately the amount of water needed for irrigation, leading to more cost-
428 effective management of the water resource.

429 Time-lapse EMI in the third case study reveals that direct drill and plow treatments influence
430 the soil moisture dynamics and the nitrogen uptake by the crop. From Figure 1c, it can be
431 observed that direct drill resulted in patchier plots mainly due to the lower survival rate of the
432 plants in the direct drill plots over winter. During the growing season, direct drill plots showed
433 a somewhat smaller rate of decrease in ECa (Figure 8). It is probably the case that the direct
434 drilled plots remained wetter due to a combination of lower evapotranspiration losses from a
435 lower leaf area (Figure 10) and a more restricted root system. This is consistent with
436 Sławiński et al. (2012) who found higher soil moisture in reduced tillage compared with

437 conventional tillage, for three years of winter wheat monoculture on two different soils. The
438 potential decrease in porosity in the plow treatment during the season could have increased
439 the ECa. However, given that a general decrease in ECa is observed, this effect is probably
440 minor compared to change in soil moisture. Nevertheless, it could potentially lead to an
441 underestimation of the soil drying in the plow treatment based on ECa changes. The addition
442 of nitrogen fertilizer caused a significant increase in ECa over a short period (Figure 6). The
443 changes in ECa correlates well with the amount of nitrogen supplied (Figure 7). This is in
444 accordance with the results of Eigenberg et al. (2002) who successfully use EMI for
445 monitoring different nitrogen uptakes. However, this effect was only observed after the first
446 application of fertilizer (2019-03-04) and not the second (2019-04-23). This could be because
447 of a more rapid nitrogen uptake due to larger plants at the second application. In contrast, the
448 LAI started to increase proportionally to the nitrogen level after the second application (Figure
449 10). This increase in LAI, potentially lead to larger soil drying and might be the cause of the
450 significant differences observed between the tillage treatments (Figure 8). Yield response to
451 the different rates was also larger for the plow than for the direct drill treatment (Figure 9).
452 One possible explanation is that the larger root impedance in direct drill treatments led to a
453 less effective use of nitrogen fertilizer (Ge et al., 2019). However, without additional nitrogen,
454 both plow and direct-drill treatments had similar yield. Overall, time-lapse EMI enables us to
455 obtain information on the soil moisture and nitrogen dynamics taking place in different tillage
456 treatments.

457 **4.2 Limitations and recommendations**

458 The cases we describe demonstrate that the minimal invasive operation of EMI and its high
459 throughput are significant advantages of this method for agricultural applications. In some

460 cases, EMI surveys can even be conducted while the crop is still in place (e.g. placing the
461 instrument between the rows of wheat or the ridges of potatoes without damaging the crop).
462 For its part, the greater resolution of ERT allows better recovery of depth-specific properties at
463 the expense of a more complex setup. The two methods have the advantage of sampling a
464 relatively large volume of soil, producing more representative measurements than
465 conventional soil sampling or soil moisture sensing. While both methods can be used for one-
466 time survey, time-lapse studies clearly have great potential for agricultural studies as they
467 enable the observation of the variation of states that can be related to plant development and
468 plant productivity.

469 EMI instruments are sensitive to measurement drift and for our case-studies we let the
470 instrument warm up to outdoor temperature for at least 30 min before starting the data
471 collection (following Shanahan et al., 2015). Additionally, the setup of a drift station, a place
472 where measurements are collected at regular time interval, is recommended. More complex
473 drift correction can also be applied (Robinson et al., 2004; Delefortrie et al., 2014). This
474 procedure is essential for time-lapse surveys as it is likely that the drift of one survey will be
475 different from another survey, inducing bias in the analysis. Temperature corrections are also
476 essential in time-lapse surveys as mentioned in section 2.4, as the soil temperature is an
477 important factor contributing to the soil EC.

478 Calibration of EMI, possibly by using an ERT array (Lavoué et al., 2010; von Hebel et al.,
479 2019), help to transform qualitative EMI data to more quantitative values. However, it requires
480 that ERT and EMI data span a sufficient range of EC values (in time or in space) in order to
481 build a strong relationship, which can be a limitation in some situation. In our case, robust
482 calibration equations were obtained for the wheat experiment using four time-lapse ERT

483 arrays across the field and using a single time-lapse ERT array for the cover-crop
484 experiments.

485 Multi-coil EMI instruments now enable the inversion of ECa data to depth-specific EC.
486 However, this inversion remains challenging given the usual small number of coil
487 configurations. Indeed, while ERT datasets usually consist of hundreds if not thousands of
488 quadrupoles providing overlapping information on the same soil volume, EMI datasets usually
489 rely on a few coil configurations. Smoothed Gauss-Newton solution (Whalley et al., 2017),
490 MCMC methods (Shanahan et al., 2015) or the shuffle complex algorithm (von Hebel et al.,
491 2014) are a few of the available methods for 1D inversion of EMI data.

492 While the above precautions are not needed with ERT instruments, the electrode setup and
493 acquisition are more important. Electrodes, after initial installation, can be left in place while
494 the crop is growing allowing time-lapse measurements to be taken at the same exact position.
495 This enables ERT surveys to be inverted using difference inversion (LaBrecque and Yang,
496 2001). The drawback of that is that soils with high clay content will tend to swell and shrink,
497 eventually leading to desiccation cracks around the electrodes (point of stress concentration)
498 undermining the galvanic contact needed for ERT acquisition. Such effects have led some
499 authors to explore the use of ERT to detect cracks in soils (Samouëlian et al., 2003;
500 Samouelian et al., 2004; Hassan and Toll, 2013). Using a mobile ERT array that is set up for
501 each survey can be an alternative but require more precautions to not damage the growing
502 crop during installation. Given that the electrodes are unlikely to be at the same exact
503 positions as previous surveys, a difference inversion cannot be used but inversion with
504 constraint to a reference dataset can be adopted (as it is the case here). Once inverted, ERT
505 sections also need to be temperature corrected.

506 Relating soil EC to soil properties or state is ultimately challenging. This is because EC is
507 influenced by many factors (texture, density, pore water EC, soil moisture, temperature).
508 These factors need to be controlled or accounted for to develop an EC value that relates the
509 property of interest. Pedophysical relationships linking geophysical properties to soil
510 properties are often site-specific and can be non-linear (Laloy et al., 2011; Calamita et al.,
511 2012). While this manuscript does not attempt to convert change in EC to soil moisture
512 content, we believe that the time-lapse approach and data processing carried out allow for the
513 previous interpretations to be made. However, if changes in other soil properties, such as the
514 decrease in porosity from tillage during the season, were to be observed with geophysical
515 instruments, independent measurements of the soil moisture variation would be needed in
516 order to better isolate the contribution of the change in porosity to the ECa variation.

517 The three case-studies presented in this work, were applied to relatively small plots from
518 research sites. However, the geophysical methods proposed, particularly EMI has the
519 potential to map much larger areas (Brogi et al., 2019). ERT systems as well, mounted on
520 towed system (e.g. Veris Quad EC 1000) also allow mapping of large area. However,
521 because ERT requires galvanic contact with the soil, it might be challenging to use a towed
522 system without damaging a growing crop.

523 Finally, other geophysical methods such as acoustic/seismic (Lu, 2014), ground penetrating
524 radar (Klenk et al., 2015; Algeo et al., 2018; Klotzsche et al., 2019; Akinsunmade et al., 2019)
525 or even nuclear magnetic resonance (Paetzold et al., 1985) are emerging methods that have
526 potential for agricultural applications.

527 **5 Conclusion**

528 Time-lapse EMI and ERT surveys detect changes in EC that can more easily be related to
529 variable states, such as soil moisture, compared to conventional static (one time) surveys.
530 The collection of case studies reported here illustrate the effectiveness of time-lapse
531 geophysics for a range of applications. The time-lapse approach helps to monitor cover crop
532 effect on soil drying and image the reduced depth of water uptake in compacted soil for
533 potatoes. Under winter wheat, a plow-based treatment showed larger decrease in ECa
534 associated with larger soil drying compared to a direct drill treatment, which might explain the
535 yield gap observed. Significant correlation between the different level of nitrogen and the ECa
536 changes was also found but only for a short period of time. In contrast, yield and LAI showed
537 a stronger response to nitrogen levels in plow than in direct drill treatment. While
538 interpretation of geophysical data should always be done carefully, we believe that the use of
539 the time-lapse approach for EMI and ERT dataset have great potential to monitor the effects
540 of a range of agricultural practices.

541 **Acknowledgments**

542 G.B. is supported by a Lancaster University - Rothamsted Research- CEH Graduate School
543 for Environment PhD studentship. M.J.H and W.R.W. at Rothamsted Research are supported
544 by the Designing Future Wheat Program by the UK Biotechnology and Biological Sciences
545 Research Council [BB/P016855/1]. One field site for the long term cover crop experiment was
546 fully funded by the British Beet Research Organisation (BBRO), the second field was funded
547 by a joint University of Nottingham [50%] – (BBRO) [50%] studentship. The work on
548 compaction and irrigation was funded under AHDB-Lancaster contracts 110002102 &
549 110002104 (Applications of precision farming technologies to enhance rotations). Pastures

550 experiment BBSRC Institute Strategic Programme grants Delivering Sustainable Systems
551 (BB/J004286/1) and Soil to Nutrition (S2N, BBS/E/C/00I0330). We are grateful for the
552 comments received from two anonymous reviewers – their input strengthened the manuscript.

553 **References**

554

- Akinsunmade, A., S. Tomecka-Suchoń, and P. Pysz. 2019. Correlation between agrotechnical properties of selected soil types and corresponding GPR response. *Acta Geophys.* doi: 10.1007/s11600-019-00349-4.
- Algeo, J., L. Slater, A. Binley, R.L. Van Dam, and C. Watts. 2018. A Comparison of Ground-Penetrating Radar Early-Time Signal Approaches for Mapping Changes in Shallow Soil Water Content. *Vadose Zone J.* 17(1): 0. doi: 10.2136/vzj2018.01.0001.
- Allred, B.J., J.J. Daniels, and M.R. Ehsani, editors. 2008. *Handbook of agricultural geophysics*. CRC Press, Boca Raton.
- Amundson, R., A.A. Berhe, J.W. Hopmans, C. Olson, A.E. Sztein, et al. 2015. Soil and human security in the 21st century. *Science* 348(6235). doi: 10.1126/science.1261071.
- Archie, G.E. 1942. The electrical resistivity log as an aid in determining some reservoir characteristics. *Trans. AIME* 146(01): 54–62.
- Batey, T. 2009. Soil compaction and soil management – a review. *Soil Use Manag.* 25(4): 335–345. doi: 10.1111/j.1475-2743.2009.00236.x.
- Binley, A. 2015. 11.08 - Tools and Techniques: Electrical Methods. In: Schubert, G., editor, *Treatise on Geophysics (Second Edition)*. Elsevier, Oxford. p. 233–259
- Binley, A., S.S. Hubbard, J.A. Huisman, A. Revil, D.A. Robinson, et al. 2015. The emergence of hydrogeophysics for improved understanding of subsurface processes over multiple scales: The Emergence of Hydrogeophysics. *Water Resour. Res.* 51(6): 3837–3866. doi: 10.1002/2015WR017016.
- Blanchy, G., S. Saneiyani, J. Boyd, P. McLachlan, and A. Binley. 2020a. ResIPy, an intuitive open source software for complex geoelectrical inversion/modeling. *Comput. Geosci.* 137: 104423. doi: 10.1016/j.cageo.2020.104423.
- Blanchy, G., C.W. Watts, R.W. Ashton, C.P. Webster, M.J. Hawkesford, et al. 2020b. Accounting for heterogeneity in the θ – σ relationship: Application to wheat phenotyping using EMI. *Vadose Zone J.* 19(1). doi: 10.1002/vzj2.20037.

- Boaga, J. 2017. The use of FDEM in hydrogeophysics: A review. *J. Appl. Geophys.* 139: 36–46. doi: 10.1016/j.jappgeo.2017.02.011.
- Brogi, C., J.A. Huisman, S. Pätzold, C. von Hebel, L. Weihermüller, et al. 2019. Large-scale soil mapping using multi-configuration EMI and supervised image classification. *Geoderma* 335: 133–148. doi: 10.1016/j.geoderma.2018.08.001.
- Calamita, G., L. Brocca, A. Perrone, S. Piscitelli, V. Lapenna, et al. 2012. Electrical resistivity and TDR methods for soil moisture estimation in central Italy test-sites. *J. Hydrol.* 454–455: 101–112. doi: 10.1016/j.jhydrol.2012.06.001.
- Calamita, G., A. Perrone, L. Brocca, B. Onorati, and S. Manfreda. 2015. Field test of a multi-frequency electromagnetic induction sensor for soil moisture monitoring in southern Italy test sites. *J. Hydrol.* 529: 316–329. doi: 10.1016/j.jhydrol.2015.07.023.
- Callegary, J.B., T.P.A. Ferré, and R.W. Groom. 2007. Vertical Spatial Sensitivity and Exploration Depth of Low-Induction-Number Electromagnetic-Induction Instruments. *Vadose Zone J.* 6(1): 158. doi: 10.2136/vzj2006.0120.
- Cimpoiașu, M.O., O. Kuras, T. Pridmore, and S.J. Mooney. 2020. Potential of geoelectrical methods to monitor root zone processes and structure: A review. *Geoderma* 365: 114232. doi: 10.1016/j.geoderma.2020.114232.
- Corwin, D.L., and S.M. Lesch. 2005. Apparent soil electrical conductivity measurements in agriculture. *Comput. Electron. Agric.* 46(1–3): 11–43. doi: 10.1016/j.compag.2004.10.005.
- Delefortrie, S., P. De Smedt, T. Saey, E. Van De Vijver, and M. Van Meirvenne. 2014. An efficient calibration procedure for correction of drift in EMI survey data. 110: 115–125. doi: 10.1016/j.jappgeo.2014.09.004.
- Doolittle, J.A., and E.C. Brevik. 2014. The use of electromagnetic induction techniques in soils studies. *Geoderma* 223–225: 33–45. doi: 10.1016/j.geoderma.2014.01.027.
- Eigenberg, R.A., J.W. Doran, J.A. Nienaber, R.B. Ferguson, and B.L. Woodbury. 2002. Electrical conductivity monitoring of soil condition and available N with animal manure and a cover crop. *Agric. Ecosyst. Environ.* 88(2): 183–193. doi: 10.1016/S0167-8809(01)00256-0.
- Fageria, N.K., V.C. Baligar, and B.A. Bailey. 2005. Role of Cover Crops in Improving Soil and Row Crop Productivity. *Commun. Soil Sci. Plant Anal.* 36(19–20): 2733–2757. doi: 10.1080/00103620500303939.
- Ge, Y., M.J. Hawkesford, C.A. Rosolem, S.J. Mooney, R.W. Ashton, et al. 2019. Multiple abiotic stress, nitrate availability and the growth of wheat. *Soil Tillage Res.* 191: 171–184. doi: 10.1016/j.still.2019.04.005.

- Hamza, M.A., and W.K. Anderson. 2005. Soil compaction in cropping systems: A review of the nature, causes and possible solutions. *Soil Tillage Res.* 82(2): 121–145.
- Hassan, A., and D.G. Toll. 2013. Electrical Resistivity Tomography for Characterizing Cracking of Soils. *Geo-Congress 2013@ Stability and Performance of Slopes and Embankments III*. ASCE. p. 818–827
- Hayashi, M. 2004. Temperature-electrical conductivity relation of water for environmental monitoring and geophysical data inversion. *Environ. Monit. Assess.* 96(1–3): 119–128.
- von Hebel, C., S. Rudolph, A. Mester, J.A. Huisman, P. Kumbhar, et al. 2014. Three-dimensional imaging of subsurface structural patterns using quantitative large-scale multiconfiguration electromagnetic induction data. *Water Resour. Res.* 50(3): 2732–2748. doi: 10.1002/2013WR014864.
- von Hebel, C., van der Kruk, J.A. Huisman, Mester, Altdorff, et al. 2019. Calibration, Conversion, and Quantitative Multi-Layer Inversion of Multi-Coil Rigid-Boom Electromagnetic Induction Data. *Sensors* 19(21): 4753. doi: 10.3390/s19214753.
- Hedley, C.B., I.J. Yule, C.R. Eastwood, T.G. Shepherd, and G. Arnold. 2004. Rapid identification of soil textural and management zones using electromagnetic induction sensing of soils. *Soil Res.* 42(4): 389. doi: 10.1071/SR03149.
- Hobbs, P.R., K. Sayre, and R. Gupta. 2008. The role of conservation agriculture in sustainable agriculture. *Philos. Trans. R. Soc. B Biol. Sci.* 363(1491): 543–555. doi: 10.1098/rstb.2007.2169.
- Jayawickreme, D.H., E.G. Jobbágy, and R.B. Jackson. 2014. Geophysical subsurface imaging for ecological applications. *New Phytol.* 201(4): 1170–1175. doi: 10.1111/nph.12619.
- Keller, T., T. Colombi, S. Ruiz, M.P. Manalili, J. Rek, et al. 2017. Long-Term Soil Structure Observatory for Monitoring Post-Compaction Evolution of Soil Structure. *Vadose Zone J.* 16(4): vzj2016.11.0118. doi: 10.2136/vzj2016.11.0118.
- Keller, T., M. Lamand, S. Peth, M. Berli, J.-Y. Delenne, et al. 2013. An interdisciplinary approach towards improved understanding of soil deformation during compaction. *Soil Tillage Res.* 128: 61–80. doi: 10.1016/j.still.2012.10.004.
- Klenk, P., S. Jaumann, and K. Roth. 2015. Quantitative high-resolution observations of soil water dynamics in a complicated architecture using time-lapse ground-penetrating radar. *Hydrol. Earth Syst. Sci.* 19(3): 1125–1139. doi: 10.5194/hess-19-1125-2015.
- Klotzsche, A., L. Lärm, J. Vanderborght, G. Cai, S. Morandage, et al. 2019. Monitoring Soil Water Content Using Time-Lapse Horizontal Borehole GPR Data at the Field-Plot Scale. *Vadose Zone J.* 18(1): 0. doi: 10.2136/vzj2019.05.0044.

- LaBrecque, D.J., and X. Yang. 2001. Difference inversion of ERT data: A fast inversion method for 3-D in situ monitoring. *J. Environ. Eng. Geophys.* 6(2): 83–89.
- Laloy, E., M. Javaux, M. Vanclooster, C. Roisin, and C.L. Bielders. 2011. Electrical Resistivity in a Loamy Soil: Identification of the Appropriate Pedo-Electrical Model. *Vadose Zone J.* 10(3): 1023. doi: 10.2136/vzj2010.0095.
- Lavoué, F., J. Van Der Kruk, J. Rings, F. André, D. Moghadas, et al. 2010. Electromagnetic induction calibration using apparent electrical conductivity modelling based on electrical resistivity tomography. *Surf. Geophys.* 8(6): 553–561.
- Lu, Z. 2014. Feasibility of Using a Seismic Surface Wave Method to Study Seasonal and Weather Effects on Shallow Surface Soils. *J. Environ. Eng. Geophys.* 19(2): 71–85. doi: 10.2113/JEEG19.2.71.
- Ma, R., A. McBratney, B. Whelan, B. Minasny, and M. Short. 2011. Comparing temperature correction models for soil electrical conductivity measurement. *Precis. Agric.* 12(1): 55–66. doi: 10.1007/s11119-009-9156-7.
- McLachlan, Paul, Guillaume Blanchy, and Andrew Binley. 2020. 'EMagPy: Open-Source Standalone Software for Processing, Forward Modeling and Inversion of Electromagnetic Induction Data'. *Computers & Geosciences*, August, 104561. <https://doi.org/10.1016/j.cageo.2020.104561>.
- Paetzold, R.F., G.A. Matzkanin, and A.D.L. Santos. 1985. Surface Soil Water Content Measurement Using Pulsed Nuclear Magnetic Resonance Techniques. *Soil Sci. Soc. Am. J.* 49(3): 537–540. doi: 10.2136/sssaj1985.03615995004900030001x.
- Rhoades, J.D., P.A.C. Raats, and R.J. Prather. 1976. Effects of liquid-phase electrical conductivity, water content, and surface conductivity on bulk soil electrical conductivity. *Soil Sci. Soc. Am. J.* 40(5): 651–655.
- Robinson, D.A., I. Lebron, S.M. Lesch, and P. Shouse. 2004. Minimizing Drift in Electrical Conductivity Measurements in High Temperature Environments using the EM-38. *Soil Sci. Soc. Am. J.* 68(2): 339–345. doi: 10.2136/sssaj2004.3390.
- Romero-Ruiz, A., N. Linde, T. Keller, and D. Or. 2018. A Review of Geophysical Methods for Soil Structure Characterization: GEOPHYSICS AND SOIL STRUCTURE. *Rev. Geophys.* doi: 10.1029/2018RG000611.
- Samouëlian, A., I. Cousin, G. Richard, A. Tabbagh, and A. Bruand. 2003. Electrical Resistivity Imaging for Detecting Soil Cracking at the Centimetric Scale. *Soil Sci. Soc. Am. J.* 67(5): 1319. doi: 10.2136/sssaj2003.1319.
- Samouëlian, A., I. Cousin, A. Tabbagh, A. Bruand, and G. Richard. 2005. Electrical resistivity survey in soil science: a review. *Soil Tillage Res.* 83(2): 173–193. doi: 10.1016/j.still.2004.10.004.

- Samouëlian, A., G. Richard, I. Cousin, R. Guerin, A. Bruand, et al. 2004. Three-dimensional crack monitoring by electrical resistivity measurement. *Eur. J. Soil Sci.* 55(4): 751–762. doi: 10.1111/j.1365-2389.2004.00632.x.
- Schlumberger, C. 1920. Etude sur la prospection électrique du sous-sol. Gauthier-Villars.
- Shanahan, P.W., A. Binley, W.R. Whalley, and C.W. Watts. 2015. The Use of Electromagnetic Induction to Monitor Changes in Soil Moisture Profiles beneath Different Wheat Genotypes. *Soil Sci. Soc. Am. J.* 79(2): 459. doi: 10.2136/sssaj2014.09.0360.
- Sławiński, C., J. Cymerman, B. Witkowska-Walczak, and K. Lamorski. 2012. Impact of diverse tillage on soil moisture dynamics. *Int. Agrophysics* 26(3): 301–309. doi: 10.2478/v10247-012-0043-5.
- Tan, X., A. Mester, C. von Hebel, E. Zimmermann, H. Vereecken, et al. 2019. Simultaneous calibration and inversion algorithm for multiconfiguration electromagnetic induction data acquired at multiple elevations. *GEOPHYSICS* 84(1): EN1–EN14. doi: 10.1190/geo2018-0264.1.
- Tang, S., A.A. Farooque, M. Bos, and F. Abbas. 2019. Modelling DUALEM-2 measured soil conductivity as a function of measuring depth to correlate with soil moisture content and potato tuber yield. *Precis. Agric.* doi: 10.1007/s11119-019-09678-2.
- Viscarra Rossel, R.A., V.I. Adamchuk, K.A. Sudduth, N.J. McKenzie, and C. Lobsey. 2011. Chapter Five - Proximal Soil Sensing: An Effective Approach for Soil Measurements in Space and Time. In: Sparks, D.L., editor, *Advances in Agronomy*. Academic Press. p. 243–291
- Waxman, M.H., and L.J.M. Smits. 1968. Electrical conductivities in oil-bearing shaly sands. *Soc. Pet. Eng. J.* 8(02): 107–122.
- Whalley, W.R., A. Binley, C.W. Watts, P. Shanahan, I.C. Dodd, et al. 2017. Methods to estimate changes in soil water for phenotyping root activity in the field. *Plant Soil* 415(1–2): 407–422. doi: 10.1007/s11104-016-3161-1.
- Wunderlich, T., H. Petersen, S. Attia al Hagrey, and W. Rabbel. 2013. Pedophysical Models for Resistivity and Permittivity of Partially Water-Saturated Soils. *Vadose Zone J.* 12(4): 0. doi: 10.2136/vzj2013.01.0023.
- Zhao, P.-F., Y.-Q. Wang, S.-X. Yan, L.-F. Fan, Z.-Y. Wang, et al. 2019. Electrical imaging of plant root zone: A review. *Comput. Electron. Agric.* 167: 105058. doi: 10.1016/j.compag.2019.105058.